SUPPLEMENTAL FIGURE LEGENDS

Figure S1, related to Figure 1. Mitochondrial morphology and connectivity in mouse skeletal muscle fibers

(A) Representative image of mitochondrial morphology in type IIX/IIB fibers from wildtype EDL muscle. Type IIX/IIB fibers were identified by conditional expression of mito-Dendra2 driven by the *Pvalb-Cre* driver. Scale bar, 20 μm. (B) Representative image of mitochondrial morphology in type I fibers (identified by expression of MyH7-CFP) in wildtype diaphragm muscle. Note that the non-CFP expressing fiber does not have elongated mitochondria in the longitudinal direction. Scale bar, 20 μm. (C) Representative image of mitochondrial morphology (visualized by mito-Dendra2 expression) in type I fibers (identified by expression of MyH7-CFP) in wildtype soleus muscle. Scale bar, 10 μm. (D) Levels of the indicated mitochondrial proteins in wild-type adult EDL (a fast twitch muscle) and soleus muscle (a slow twitch muscle), as measured by Western blot.

Figure S2, related to Figure 4. Mitochondrial function in glucose vs. acetoacetate-media

(A) Representative images of mitochondrial membrane potential (TMRM staining) in the indicated media condition. Scale bar, 10 μm. (B) Quantification of membrane potential (TMRM staining) in the indicated media condition. Error bars indicate standard deviation. Experiments were performed in triplicate. (C) Representative data of oxygen consumption from intact muscle in glucose-media. Drugs were added at the times indicated by the arrows. Oxygen consumption rates (OCRs) were calculated as the slope of oxygen versus time. (D) Quantification of basal OCR, maximal (CCCP-stimulated) OCR, and cellular RCR (respiratory control ratio = maximal OCR / oligomycin-inhibited OCR) in the indicated media conditions. Error bars indicate

standard deviation. Experiments were performed in triplicate. (E) Photoconversion of mito-Dendra2 in type IIX/IIB fibers from an *ex vivo* EDL muscle, subject to overnight culturing in the indicated media condition. The red box indicates the photoconverted region of interest. Scale bar, 2 μm.

Figure S3, related to Figure 5. Stochastic labeling of individual myonuclei in mouse skeletal muscle

(A) Representative image of a mito-Dendra2 expressing satellite cell that has not fused with its adjacent myofiber. Scale bar, 20 μm. (B) Representative image of mito-Dendra2 expression within a myofiber, after fusion of labeled satellite cell. Scale bar, 20 μm. (C) Representative images of a single mitochondrial domain (left) and a dual mitochondrial domain (right). Scale bar, 20 μm. For each myofiber, total vertical fluorescence intensity (green) is plotted as a function of longitudinal axis (below). Moving average of fluorescence intensity is shown in solid black. (D) Individual z-slices of a mitochondrial domain taken at the top, middle and bottom of a myofiber. Scale bar, 20 μm. (E2) Fluorescence intensity (moving average) is plotted versus distance for the three z-slices shown in (E). (F) Nuclear GFP fluorescence in a *Pax7-CreERT2; nuclear-GFP*^{cond} myofiber. GFP immunostaining identifies a single, labeled nucleus within the myofiber. Scale bar, 20 μm.

Figure S4, related to Figure 6. Stability of mitochondrial domains

(A) Representative images of a mitochondrial domain in an *ex vivo* cultured myofiber at the indicated time points. Scale bar, 20 μm. (B) Quantification of mitochondrial domain size over time during *ex vivo* culturing. Data is normalized to domain size at time t=0 hr. Error bars

indicate standard errors for n>10 fibers. (C) Representative low-magnification tiled images of mitochondrial domains from a young and adult animal. Scale bar, 200 μm. (D) Quantification of domain frequency, calculated as number of domains per 1000 μm of fiber length, for animals of the indicated ages. At least 50 domains per group were quantified. *, $p<0.05$; **, $p<0.01$; (t-test). Error bars indicate standard errors. (E) Domain size in the indicated fiber types and tissues from wildtype animals. At least 30 domains per group were quantified. *, $p<0.001$ (t-test). Error bars indicate standard errors.

Figure S1

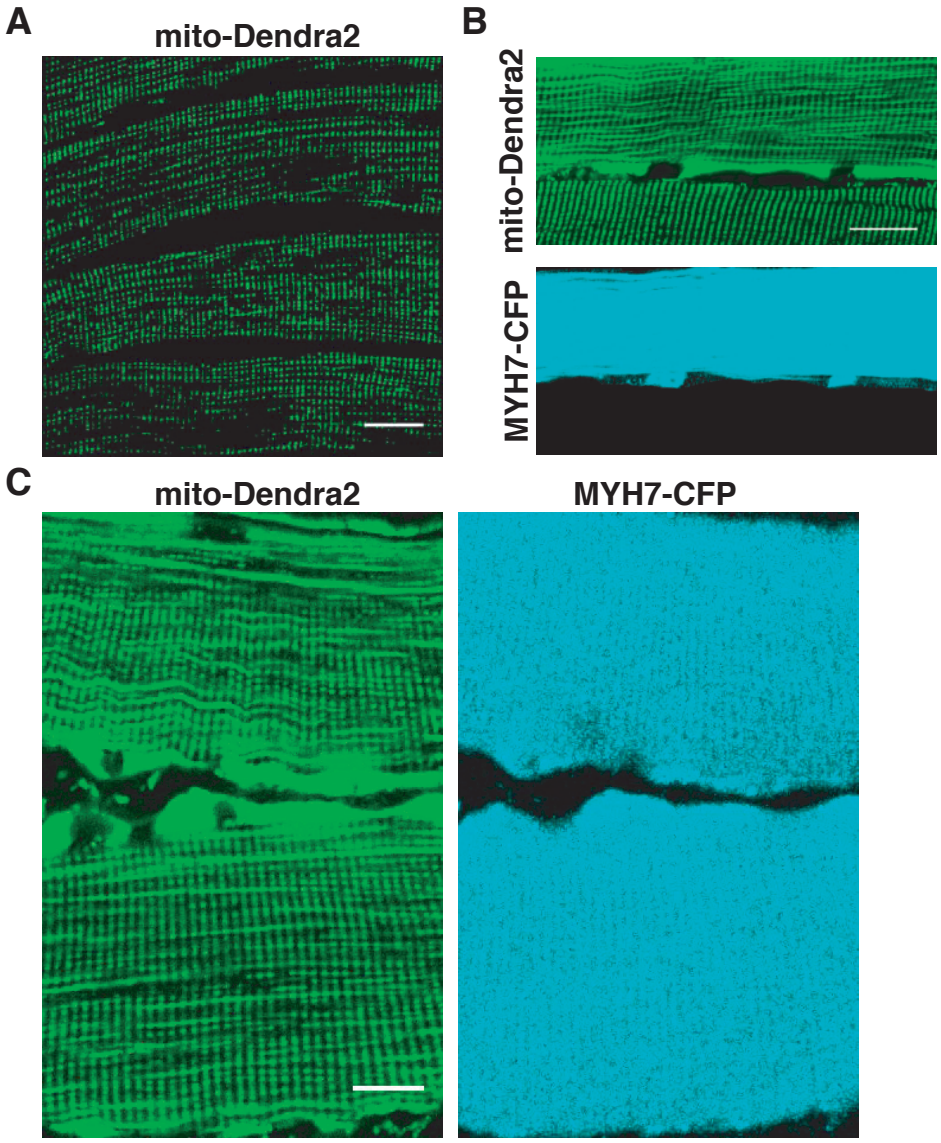
A
mito-Dendra2
B
mito-Dendra2
MYH7-CFP
C
mito-Dendra2
MYH7-CFP
D
sol
EDL
Mfn1
Mfn2
Mff
Hsp60
Tom20

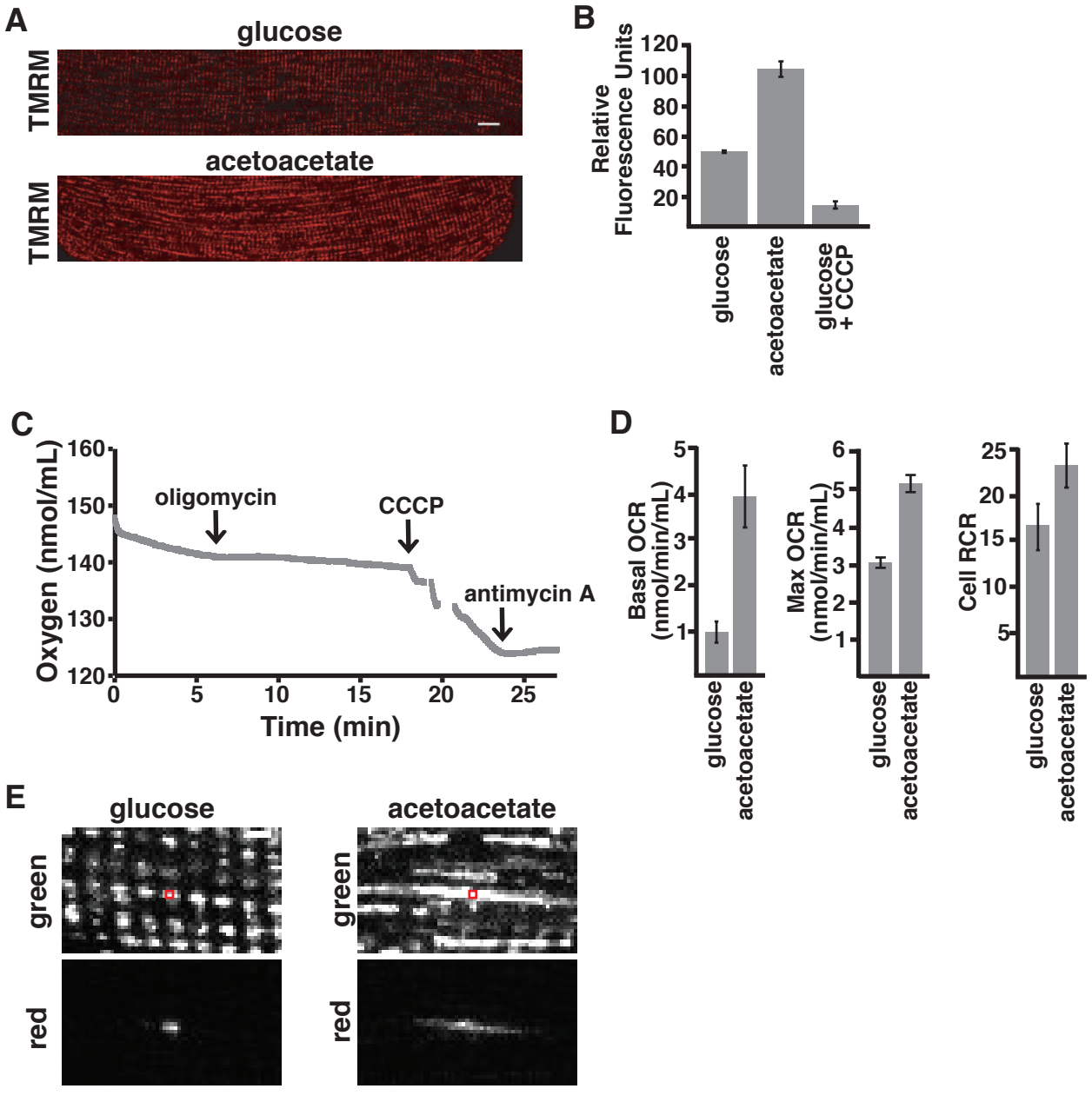
A
glucose
TMRM
acetoacetate
TMRM
B
Relative Fluorescence Units
120
100
80
60
40
20
glucose
acetoacetate
glucose + CCCP
C
Oxygen (nmol/mL)
160
150
140
130
120
oligomycin
CCCP
antimycin A
0
5
10
15
20
25
Time (min)
D
Basal OCR (nmol/min/mL)
5
4
3
2
1
glucose
acetoacetate
Max OCR (nmol/min/mL)
6
5
4
3
2
1
glucose
acetoacetate
Cell RCR
25
20
15
10
5
glucose
acetoacetate
E
glucose
acetoacetate
green
red
green
red

Figure S3

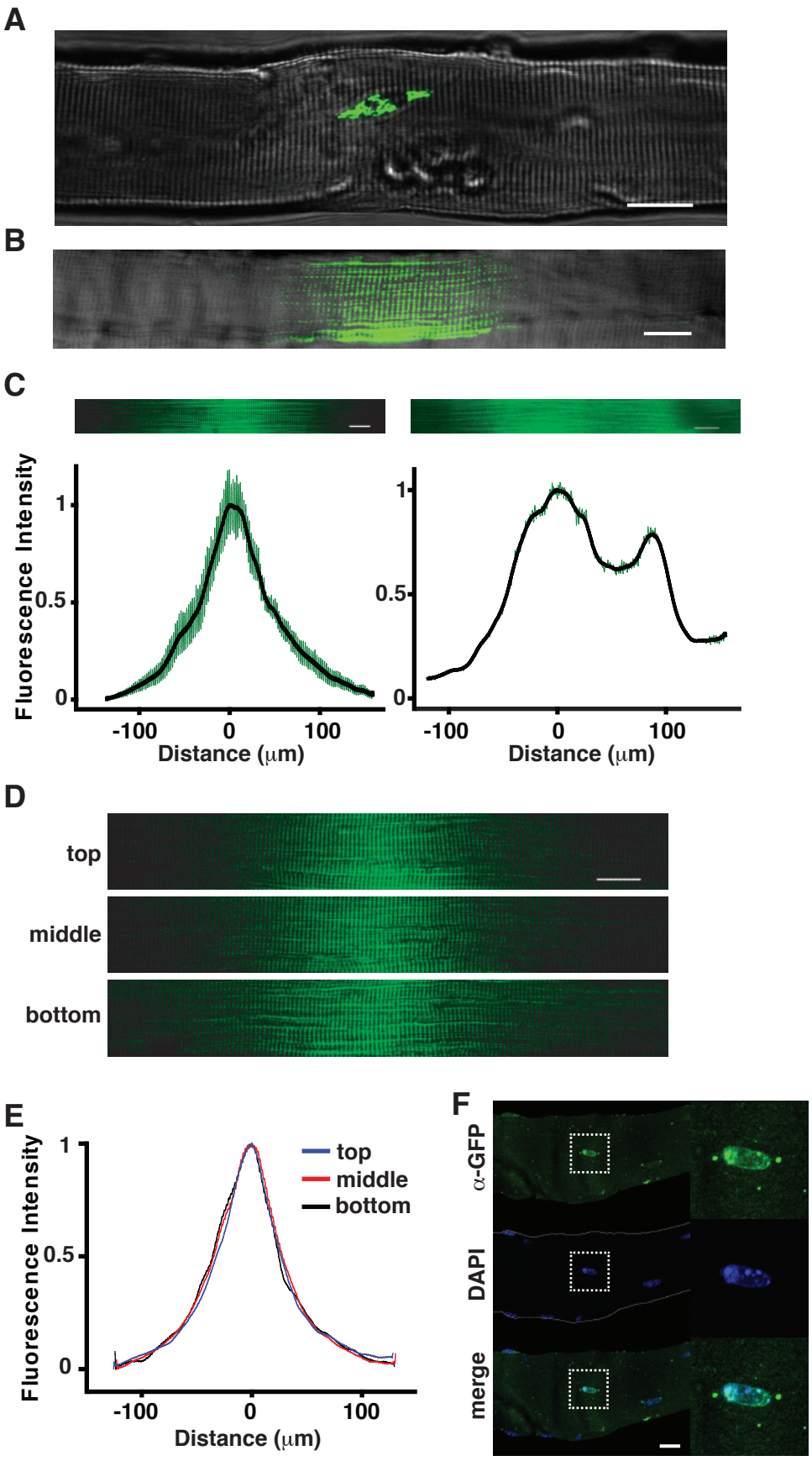
A
B
C
Fluorescence Intensity
1
0.5
0
-100
0
100
Distance (μm)
D
top
middle
bottom
E
Fluorescence Intensity
top
middle
bottom
Distance (μm)
F
α-GFP
DAPI
merge

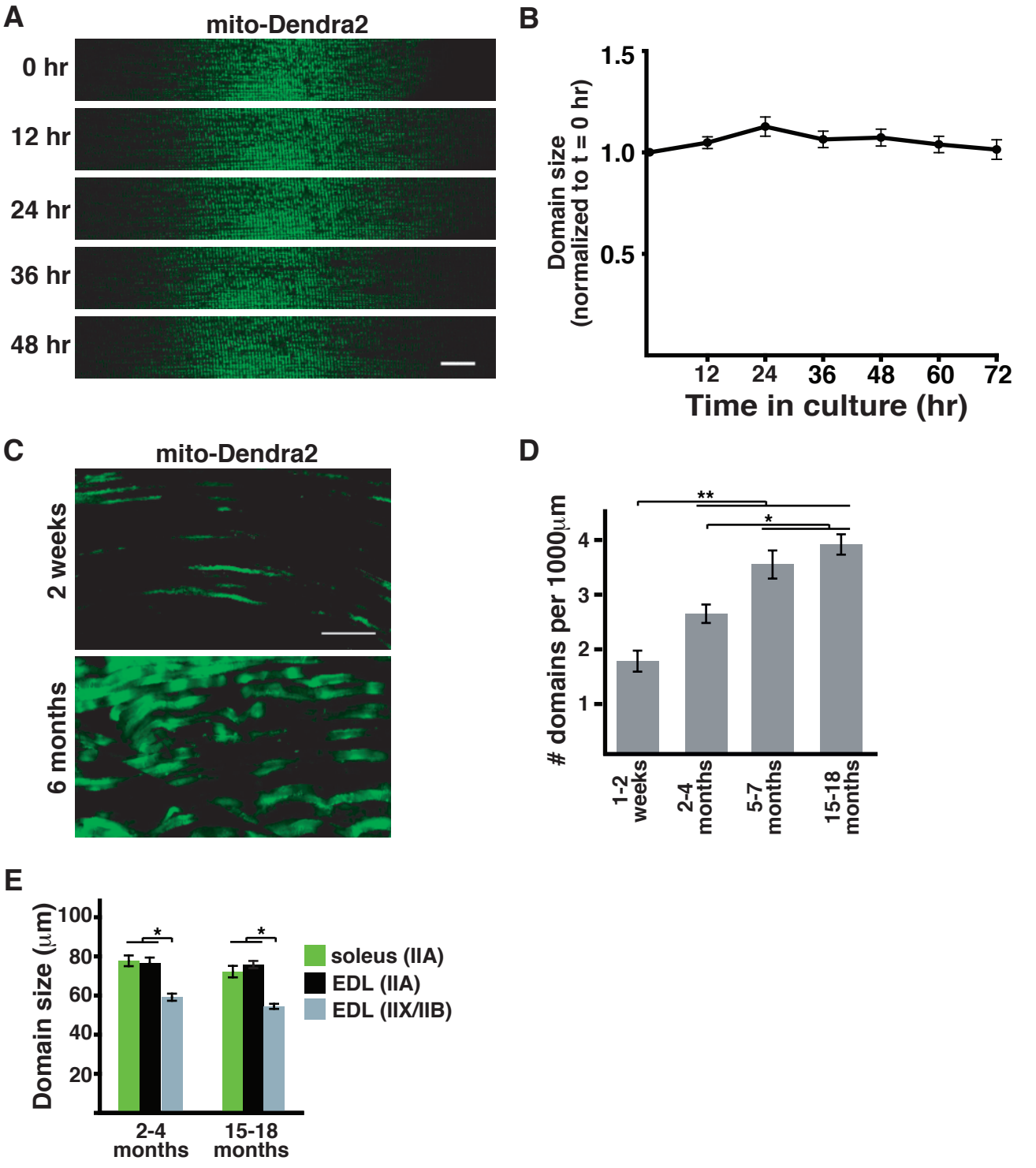
A
mito-Dendra2
0 hr
12 hr
24 hr
36 hr
48 hr
B
Domain size (normalized to t = 0 hr)
1.5
1.0
0.5
12
24
36
48
60
72
Time in culture (hr)
C
mito-Dendra2
2 weeks
6 months
D
domains per 1000μm
**
*
4
3
2
1
1-2 weeks
2-4 months
5-7 months
15-18 months
E
Domain size (μm)
100
80
60
40
20
*
*
soleus (IIA)
EDL (IIA)
EDL (IIX/IIB)
2-4 months
15-18 months